

From the Tully-Fisher relation to the Fundamental Plane through Mergers

Héctor Aceves* and Héctor Velázquez

Instituto de Astronomía, Universidad Nacional Autónoma de México, Apdo. Postal 877, Ensenada, BC 22800, México

Accepted — . Received —; in original form —

ABSTRACT

We set up a series of self-consistent N -body simulations to investigate the fundamental plane of merger remnants of spiral galaxies. These last ones are obtained from a theoretical Tully-Fisher relation at $z=1$, assuming a constant mass-to-light ratio within the Λ CDM cosmogony. Using a Sérsic growth curve and an orthogonal fitting method, we found that the fundamental plane of our merger remnants is described by the relation $R_e \propto \sigma_0^{1.48 \pm 0.01} I_e^{-0.75 \pm 0.01}$ which is in good agreement with that reported from the Sloan Digital Sky Survey $R_e \propto \sigma_0^{1.49 \pm 0.05} I_e^{-0.75 \pm 0.01}$. However, the $R^{1/4}$ -profile leads to a fundamental plane given by $R_e \propto \sigma_0^{1.79 \pm 0.01} I_e^{-0.60 \pm 0.01}$. In general, the correlation found in our merger remnants arises from homology breaking ($V^2 \propto \sigma_0^\nu$, $R_g \propto R_e^\eta$) in combination with a mass scaling relation between the total and luminous mass, $M \propto M_L^\gamma$. Considering an orthogonal fitting method, it is found that $1.74 \lesssim \nu \lesssim 1.79$, $0.21 \lesssim \eta \lesssim 0.52$ and $0.80 \lesssim \gamma \lesssim 0.90$ depending on the adopted profile (Sérsic or $R^{1/4}$).

Key words: galaxies: formation – galaxies: fundamental parameters – galaxies: elliptical – methods: N -body simulations.

1 INTRODUCTION

The formation and evolution of elliptical galaxies continues to be an outstanding problem in astrophysics (e.g. Meza et al. 2003, Wright et al. 2003). In the current CDM models of hierarchical structure formation, mergers are the common process through which larger objects form from small ones (Frenk et al. 1988, Kauffmann & White 1993, Lacey & Cole 1993). In this scenario, ellipticals are a ‘natural’ outcome (Toomre 1977) and accumulating observational evidence seems to support this (Schweizer 1998 and references therein). However, an important challenge to the merger hypothesis is to explain how this seemingly random merging process can lead to the tight correlations found in ellipticals (White 1997).

One of this correlations found in ellipticals is the so-called Fundamental Plane (FP); a linear relation, in the logarithmic space, among their effective radius, R_e , their effective surface brightness, I_e , and their one-dimensional central velocity dispersion, σ_0 (Djorgovski & Davis 1987; Dressler et al. 1987): $R_e \propto \sigma_0^a I_e^b$. The FP exhibits a general trend that follows from the application of the virial theorem to ellipticals: $M \propto V^2 R_g$, with M being the total mass, V^2 the 3-dimensional mean square velocity and R_g the gravitational radius of the system ($V^2 = 2K/M$ and $R_g = GM^2/|W|$, where K and W are the total kinetic and potential energy, respectively). Assuming that ellipticals are homologous systems in equi-

librium ($V^2 \propto \sigma_0^2$, $R_g \propto R_e$) with a constant mass-to-light ratio, the virial theorem leads to

$$R_e \propto \sigma_0^2 I_e^{-1} \rightarrow \log R_e \approx 2[\log \sigma_0 + 0.2\mu_e] \quad (1)$$

where $\mu_e = -2.5 \log I_e$. Deviations of an observed FP from the theoretical expectation are attributed to variations of the mass-to-light ratio with luminosity and/or to the breaking of homology in galaxies (e.g. Trujillo, Burkert & Bell 2004).

The observed FP presents some differences depending on the wave-band spectrum and on the environment where galaxies reside (Jørgensen et al. 1996; Pahre et al. 1998; Mobasher et al. 1999; Kelson et al. 2000; Bernardi et al. 2003). Recently, from a sample of about 9000 elliptical galaxies taken from the Sloan Digital Sky Survey (SDSS), Bernardi et al. (2003) obtained a FP relation given by $R_e \propto \sigma_0^{1.49 \pm 0.05} I_e^{-0.75 \pm 0.01}$; where the $R^{1/4}$ -profile was assumed.

On the theoretical side, simulations of spiral mergers are numerous and have been extensively explored to study: the morphology of merger remnants (e.g. Mihos & Hernquist 1996), the line-of-sight velocity distribution (e.g. Bendo & Barnes 2000), and the effect of the orientation of the angular momentum of discs (e.g. Naab & Burkert 2003). Other works have considered the effect of mergers on the properties of the FP (e.g. Capelato et al. 1995, Levine & Aguilar 1996, Bekki 1998, Dantas et al. 2003, Nipoti et al. 2003, González-García & van Albada 2003). A common feature of previous studies is that they have used models with properties chosen rather arbitrary resembling present day spiral galaxies. In partic-

* E-mail: aceves@astro.unam.mx

ular, those works addressing the FP of merger remnants have not considered self-consistent models of disc galaxies.

Disc galaxies also define a tight correlation between the maximum of their rotation velocity V_m and their luminosity, termed the Tully-Fisher (TF) relation, that can be written as $L = AV_m^\alpha$; where α and A are the ‘slope’ and the zero-point, respectively. The observed values for α lie between ≈ 2.5 -4, depending on the wave-band (e.g. Strauss & Willick 1995). In particular, the I -band TF relation is given by

$$M_I - 5 \log h = -21.00 - 7.68(\log W - 2.5) \quad (2)$$

where M_I is the absolute magnitude of the disc, and $W \approx 2V_m$ is the 21-cm hydrogen line width resulting in a slope of $\alpha \approx 3.1$ (Giovanelli et al. 1997).

In this *Letter* we study whether merger remnants of self-consistent N -body spirals satisfying the TF relation can lead to the FP of ellipticals. Spirals properties are obtained from the Press-Schechter formalism (Press & Schechter 1974) in combination with the model of disc galaxy formation of Mo, Mao & White (1998, hereafter MMW) and the TF relation under the Λ CDM model. The rest of this work has been structured as follows: in §2 we summarise the model used to set up the theoretical TF relation, the initial conditions and the orbital parameters for our simulations. In §3 the results and a discussion are given.

2 NUMERICAL MODEL

In this section we summarise the method and properties of our models to study the FP associated to merger remnants.

2.1 Tully-Fisher relation of spirals

To construct a theoretical TF we use the Press-Schechter framework of hierarchical clustering and the model of MMW for the formation of galaxy discs. In this model five parameters are required to obtain the radial scale-length of a disc formed inside a spherical dark halo. These are the circular velocity, V_c , the spin parameter, λ , the concentration of the halo, c , the fraction of disc to halo mass, m_d and the fraction of angular momentum in the disc, j_d . To obtain $(V_c, \lambda, c, m_d, j_d)$ we have proceeded as in Shen, Mo & Shu (2002). The Λ CDM cosmology was adopted to obtain the particular properties of disc galaxies (with a mass density parameter of $\Omega_0=0.3$, a cosmological constant of $\Omega_\Lambda=0.7$, the Hubble’s constant $h=0.7$, and the perturbation power-spectrum normalization $\sigma_8=1$).

We have used the theoretical TF at $z=1$, an epoch thought to be close to the one where formation of the discs occurred (Peebles 1993), as our fiducial redshift to construct the numerical disc galaxies. This allowed us to consider remnants resulting from binary encounters and to compare them with ellipticals that might have formed through these encounters. Present day massive ellipticals are probably the result of more than a binary merger, but their study is out of the scope of this work.

We have selected only disc galaxies with a stability criterion $\epsilon_m \geq 0.9$, where $\epsilon_m = V_m (GM_d/R_d)^{-1/2}$, and V_m is the maximum rotation velocity (Efstathiou, Lake & Negroponte 1982; Syer, Mao & Mo 1997). Galaxies were evolved in isolation during 2 Gyr, about twice the time needed for the first pericentric passage in the encounter. Despite the fact that our galaxy models match the previous criterion some form a well defined bar (B) while in other cases they develop a transient bar (T) or remain stable (S) (see last column of Table 1).

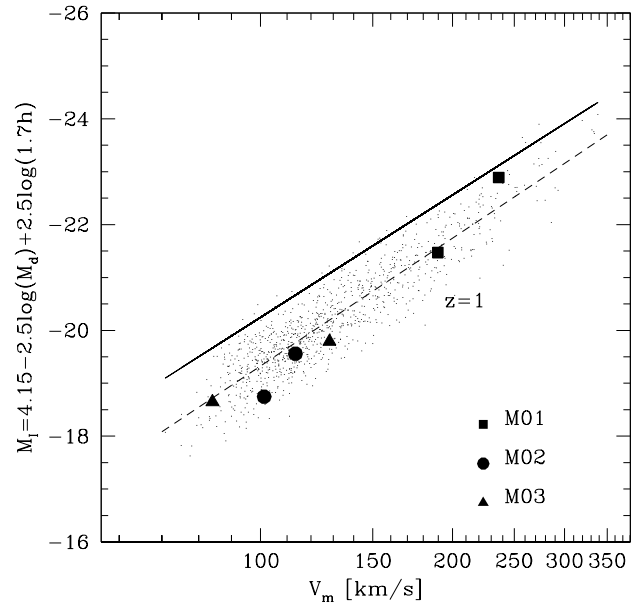


Figure 1. Theoretical Tully-Fisher relation for an ensemble of spirals (dots) at $z=1$. The dashed and solid lines correspond to the linear-square fit with a slope of $\alpha = -8.0$ and to the observed relation (2), respectively. The properties of discs of galaxies to be merged were selected from this ensemble. As an illustration, progenitors of mergers $M01$, $M02$ and $M03$ of Table 1 are shown.

In Figure 1 the TF relation, at redshift $z=1$, is shown. The straight solid line indicates the observed slope of the TF in the I -band of equation (2) at the present epoch. A sample of twenty random points from this TF relation were selected in order to set up the self-consistent N -body disc galaxies.

2.2 Galaxy models

Our N -body disc galaxy models consist of a disc and a spherical dark halo component. Following Hernquist (1993), disc particle positions are randomly drawn from the axisymmetric density profile:

$$\rho_d(R, z) = \frac{M_d}{4\pi R_d^2 z_d} \exp(-R/R_d) \operatorname{sech}^2(z/z_d), \quad (3)$$

being R_d and z_d the radial and vertical scale length of the disc, respectively; z_d was chosen randomly in the range $(0.1-0.2)R_d$. For the halo we have adopted a modified version of the NFW-profile (Navarro, Frenk & White 1997) with an exponential cut-off given by:

$$\rho_h(r) = \frac{M_h \alpha_h}{4\pi r(r+r_s)^2} \exp\left[-\left(\frac{r}{r_{200}} + q\right)^2\right], \quad (4)$$

with

$$\alpha_h = \frac{\exp(q^2)}{\sqrt{\pi} q \exp(q^2) \operatorname{Erfc}(q) + \frac{1}{2} \exp(q^2) E_1(q^2) - 1},$$

being $\operatorname{Erfc}(x)$ the complementary error function and $E_1(x)$ the exponential integral, r_s and r_{200} the scale and virial radii of the halo respectively, $c = q^{-1} = (r_s/r_{200})^{-1}$ the halo concentration, and M_h is the halo total mass. Finally, velocities are derived from Jeans equations.

The parameters characterizing our disc galaxy models are listed in Table 1; where $f_d = M_d/(M_h + M_d)$. We have also in-

Table 1. Properties of merging galaxies.

Merger	Halo Properties						Disc Properties						
	M_h [M_\odot]	r_{200} [kpc]	λ	j	c	N_h	f_d	R_d [kpc]	z_d [kpc]	Q	R_Q [kpc]	N_d	
M01	4.02×10^{11}	104.3	0.063	0.041	7.63	57126	0.0498	2.4	0.39	0.402	5.8	12000	T
	1.25×10^{12}	152.3	0.056	0.068	3.84	177571	0.0586	5.7	0.47	0.321	13.8	44267	T
M02	1.39×10^{11}	73.3	0.021	0.052	8.94	172403	0.0312	1.2	0.12	0.651	3.0	57436	T
	6.45×10^{10}	56.7	0.028	0.033	6.61	80000	0.0236	1.3	0.13	1.302	3.1	20000	S
M03	8.65×10^{10}	62.6	0.078	0.033	11.12	149138	0.0402	1.7	0.20	0.995	4.1	42093	S
	4.64×10^{10}	50.8	0.031	0.043	12.38	80000	0.0357	0.7	0.12	0.789	1.8	20000	B
M04	2.36×10^{11}	87.4	0.036	0.029	9.17	80000	0.0393	1.1	0.19	0.387	2.6	20000	T
	1.75×10^{11}	79.2	0.048	0.054	5.29	59428	0.0372	3.3	0.58	1.064	8.0	15671	S
M05	5.42×10^{10}	53.5	0.053	0.114	15.95	74829	0.0817	1.2	0.19	0.561	2.8	20000	B
	6.02×10^{10}	55.4	0.034	0.077	12.05	83124	0.0541	1.0	0.14	0.610	2.3	14245	S
M06	7.49×10^{10}	59.6	0.098	0.059	7.91	91546	0.0638	2.5	0.35	0.943	6.1	25000	B
	6.68×10^{10}	57.4	0.078	0.043	13.32	81742	0.0420	1.9	0.23	1.253	4.5	14327	S
M07	4.88×10^{10}	51.7	0.074	0.064	11.02	73643	0.0635	1.5	0.25	0.841	3.6	20000	B
	9.48×10^{10}	64.5	0.047	0.103	11.79	143062	0.0656	1.6	0.31	0.579	3.9	42119	B
M08	9.77×10^{10}	65.2	0.032	0.034	6.56	245462	0.0239	1.7	0.20	1.261	4.1	36000	S
	1.02×10^{11}	66.1	0.023	0.012	7.80	188124	0.0127	0.9	0.12	1.217	2.2	19725	S
M09	8.11×10^{10}	61.2	0.099	0.142	10.87	150000	0.0818	4.6	0.73	1.217	11.1	30000	S
	8.33×10^{10}	61.8	0.122	0.095	10.01	154050	0.0791	3.9	0.56	1.089	9.6	29686	S
M10	4.74×10^{11}	110.3	0.112	0.106	11.39	240000	0.0807	6.6	1.29	0.576	15.9	60000	B
	6.99×10^{10}	58.3	0.071	0.035	9.94	165992	0.0396	1.6	0.19	1.092	3.9	48689	S

cluded the radius R_Q at which Toomre's Q parameter is normalized and the number of particles in the halo, N_h , and the disc, N_d . Notice the range of concentrations of haloes and galaxy disc sizes.

Our disc galaxy models do not include a central bulge component since, in the framework of MMW's galaxy formation, they tend to produce smaller disc sizes which require a better spatial resolution and smaller timesteps and, hence, more demanding computational resources. It is not clear how this central component will affect the FP of the remnants; it will be addressed in a future work.

2.3 Initial conditions and experiments

We have considered only parabolic encounters where the initial separation between galaxy centres is $R_s = 1.25(r_{200,1} + r_{200,2})$. The pericentre for each encounter is randomly selected in the interval $R_p \in (5, 20)$ kpc, consistent with the energies and eccentricities of cosmological N -body simulations (Navarro, Frenk & White 1995). The relative orientation between galaxy spins is also taken randomly.

To evolve the numerical simulations we use the parallel version of GADGET, an N-body/SPH code with individual timesteps (Springel, Yoshida & White 2001). Softening parameters of $\epsilon_d=35$ pc and $\epsilon_h=350$ pc were used for the disc and the halo particles, respectively. GADGET uses a spline kernel for the softening, so that the gravitational interaction between two particles is fully Newtonian for separations larger than twice the softening parameter (Power et al. 2003).

The typical time of arrival at pericentre is about 1 Gyr, and all simulations were run for a total time of about 8 Gyr; this corresponds to about the time span from $z=1$ to $z=0$ in a Λ CDM sce-

nario. Remnants are already in a virial state by this time. All of our runs were performed on a cluster consisting of 32 Pentium processors running at 450 MHz (Velázquez & Aguilar 2003). Energy conservation was better than 0.25% in all cases.

3 RESULTS AND DISCUSSION

To analyse the merger remnants a constant mass-to-light ratio, Υ , is assumed; hence I_e is proportional to the effective surface luminous-mass density Σ_e . We first compute their 'photometric' properties (R_e, Σ_e) and then its central velocity dispersion σ_0 inside an aperture of radius $R_e/8$. The surface density profiles $\Sigma(R)$ were fitted using a Sérsic profile (Sérsic 1968; Ciotti & Bertin 1999; Caon, Capaccioli & D'Onofrio 1993) and the $R^{1/4}$ profile, we also fitted the corresponding growth curves of the luminous part of the remnants: $M_L(R) = 2\pi \int \Sigma(R) R dR$.

To check how the photometric properties are affected by the adopted region to be fitted, we have considered an aperture with outer radius of 17.5 kpc as in Wright et al (2003) and for the inner radius of the fit, ξ , we use two different values: (1) the resolution of the luminous component in our simulations, $\xi \approx 2.8\epsilon_d \approx 100$ pc, and (2) $\xi=300$ pc. This also allows us to test the effects of the boundaries of the fitting region on the values of the exponents (a, b) of the FP ($R_e \propto \sigma_0^a \Sigma_e^b$). Each remnant was 'observed' from 100 random line-of-sights. A χ^2 -minimisation by Levenberg-Marquart method (Press et al. 1992) was used to obtain R_e and Σ_e for each projection. The exponents (a, b) of the FP were fitted to the complete set of projected values of the remnants, using both orthogonal and direct fits.

The resulting values for these exponents are plotted in Fig-

Table 2. Mean of projected values used to determine our FP_f .

Merger	$\langle n \rangle$	Parameters*		
		$\langle R_e \rangle$ [kpc]	$\langle \sigma_0 \rangle$ [km/s]	$\langle \mu_e \rangle$
M01	4.3	9.0	139	-19.4
M02	2.2	2.5	75	-19.4
M03	1.8	2.2	72	-19.4
M04	2.6	3.7	95	-19.4
M05	3.8	1.7	71	-20.3
M06	2.3	3.7	67	-18.8
M07	3.2	2.5	66	-19.8
M08	2.8	2.1	45	-19.1
M09	2.1	6.1	72	-18.3
M10	2.6	5.2	71	-18.7

* Here n is the index of the Sérsic profile [$\propto \exp(-R^{1/n})$], and $\mu_e = -2.5 \log \Sigma_e$ with Σ_e in M_\odot/kpc^2 .

ure 2 (*left panel*). It can be seen how the values of parameters (a, b) are sensitive to the fitting function (profile or growth curve), to the adopted profile (Sérsic or $R^{1/4}$), to the fitting method (direct or orthogonal) and to the value of the radius ξ . The observed values in the r^* -band of the SDSS have also been included (star symbols). In particular, the dotted lines refer to the exponents of the FP of Bernardi et al. (2003): $R_e \propto \sigma_0^{1.49} I_e^{-0.75}$.

This last relation is quite well reproduced by the model with $\xi=100$ pc, a Sérsic growth curve and an orthogonal fitting method (hereafter our fiducial model, denoted by FP_f) which is expressed by the relation $R_e \propto \sigma_0^{1.48 \pm 0.01} \Sigma_e^{-0.75 \pm 0.01}$ with a standard deviation orthogonal to the plane of 0.06. Uncertainties in the exponents were estimated using the bootstrap technique (Efron & Tibshirani 1993). Table 2 lists the mean projected values of the quantities used to compute our FP_f and the mean Sérsic index.

However, the exponents (a, b) obtained by fitting the merger remnants with the $R^{1/4}$ -profile have problems matching the observed ones, and this is independent of the fitting method (orthogonal or direct). For example, for $\xi = 100$ pc and an orthogonal fitting, the $R^{1/4}$ -profile leads to a FP described by $R_e \propto \sigma_0^{1.79 \pm 0.01} \Sigma_e^{-0.60 \pm 0.01}$ (which will be denoted by FP_{dV}), while for $\xi = 300$ pc it is given by $R_e \propto \sigma_0^{1.65 \pm 0.01} \Sigma_e^{-0.65 \pm 0.01}$; notice that increasing ξ tends to provide a slight better fit. An edge-view of our FP_f for the merger remnants (filled squares) is shown in Figure 2 (*right panel*). As a reference, the long-dashed line indicates the slope, $\alpha_V = 2$, for virialised homologous systems with a constant mass-to-light ratio while the solid and dotted lines refer to the SDSS and to our FP_f , respectively. Our merger remnants were artificially displaced to coincide with the zero-point of the FP of the SDSS (Bernardi et al. 2003).

The overall agreement of the parameter values (a, b) for the Sérsic profile case with those of the SDSS relies on a combination of homology breaking ($V^2 \propto \sigma_0^a, R_g \propto R_e^b$) and a mass scaling relation between the total and luminous mass as $M \propto M_L^c$. For instance, for our FP_f non-homology is found to be $V^2 \propto \sigma_0^{1.74}$ and $R_g \propto R_e^{0.51}$, with a mass scaling relation given by $M \propto M_L^{0.85}$ and a negligible dependence of Sérsic's index with the effective radius ($n \propto R_e^{0.07}$), while for the FP_{dV} case, these relations are described by $V^2 \propto \sigma_0^{1.77}$, $R_g \propto R_e^{0.21}$ and $M \propto M_L^{0.80}$. Note that a direct fitting method shows larger differences between our fitted FP and that of the SDSS (see Figure 2-*right panel*). Despite that Sérsic's profile fitting leads to a better match with observations; a

consistent comparison will require an observational FP determined using this type of profile on the large data base of the SDSS.

The above results suggest that, ignoring any contribution from breaking-homology relations, it does not appear feasible to scale the mass-to-light ratio, (M/L), as a simple power-law of the luminosity, L , (or equivalently of the mass M) alone; see also Bernardi et al. (2003). Perhaps, a more general relation of the form $(M/L) \propto R_e^x \sigma_0^y L_e^z$ need to be explored. A more extensive study of the scaling relations of merger remnants, their non-homology, the distribution of luminous and dark matter, and their kinematics is under way and it will be presented in a future work.

Our results support the idea that mergers of spirals, with properties obtained from the Tully-Fisher relation within a Λ CDM cosmogony, lead to the tight correlation expressed by the FP.

In dissipational numerical simulations of mergers, it is found that a gas component can yield important differences in the stellar component of the remnants in comparison with their collisionless counterparts (e. g., Barnes & Hernquist 1996). For instance, a gas component deepens the potential well, affecting more the remnant kinematics than its luminous profile. However, it is not clear from these results how the FP is going to be altered; in particular, if its slope is going to be changed or just the dispersion of values around it. This remains an open issue.

ACKNOWLEDGMENTS

We thank Luis Aguilar and Simon White for their helpful comments on this work. This research was funded by CONACyT-México Project 37506-E. An anonymous referee is thanked for useful comments that helped to clarify some points of this work.

REFERENCES

- Barnes J. E., Hernquist L., 1996, ApJ, 471, 115
 Bekki K., 1998, ApJ, 496, 713
 Bendo G. J., Barnes J. E., 2000, MNRAS, 316, 315
 Bernardi M., et al., 2003, AJ, 125, 1866
 Caon N., Capaccioli M., D'Onofrio M., 1993, MNRAS, 265, 1013
 Capelato H. V., de Carvalho R. R., Carlberg R. G., 1995, ApJ, 451, 525
 Ciotti L., Bertin G., 1999, A&A, 352, L13
 Dantas, C. C., Capelato, H. V., Ribeiro, A. L. B., de Carvalho, R. R., 2003, MNRAS, 340, 398
 Djorgovski S., Davis M., 1987, ApJ, 313, 59
 Dressler A., Lynden-Bell D., Burstein D., Davis R., Faber S. M., Terlevich R., Wegner G., 1987, ApJ, 313, 42
 Efron B., R. J. Tibshirani R. J., 1993, An Introduction to the Bootstrap. Chappman & Hall., New York.
 Efstathiou G., Lake G., Negroponte J., 1982, MNRAS, 199, 1069
 Frenk C. S., White S. D. M., Davis M., Efstathiou G., 1988, ApJ, 327, 507
 Giovanelli R., Haynes M. P., da Costa L. N., Freudling W., Salzer J. J., Wegner G., 1997, ApJ, 477, L1
 González-García A. C., van Albada T. S., 2003, MNRAS, 342, L36
 Hernquist L., 1993, ApJS, 86, 389
 Jørgensen I., Franx M., Kjaergaard P., 1996, MNRAS, 280, 167
 Kauffmann G., White S. D. M., 1993, MNRAS, 261, 921
 Kelson D. D., Illingworth G. D., van Dokkum P. G., Franx M., 200, ApJ, 531, 184

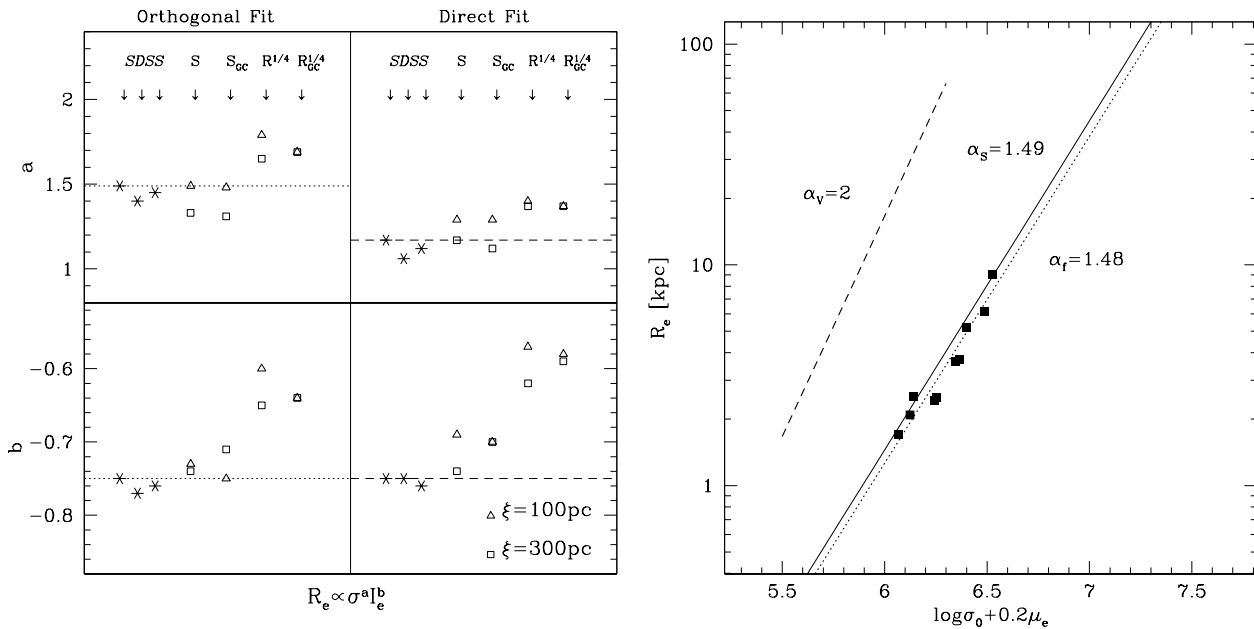


Figure 2. (Left) Parameters (a, b) for the FP ($R_e \propto \sigma_0^a I_e^b$) of our galaxy merger remnants. For comparison purposes, the values of the SDSS (star symbols) in the r^* -band have been included. Horizontal dotted lines indicate the FP relation, $R_e \propto \sigma_0^{1.49} \Sigma_e^{-0.75}$, quoted by Bernardi et al. (2003). To the left, these parameters were obtained using an orthogonal fitting method while to the right using a direct one. Here, S=Sérsic profile, S_{GC} =Sérsic's growth curve, $R^{1/4}$ =de Vaucouleurs profile, and $R_{GC}^{1/4}$ its growth curve. Also, the effect introduced by two values of the inner radii ξ is illustrated. (Right) Edge-on view of the FP. Remnants are indicated by filled squares using the mean values listed in Table 2. The solid and dotted lines correspond to the SDSS FP ($R_e \propto \sigma_0^{1.49} \Sigma_e^{-0.75}$) and to our FP_f model. As a reference, the dashed line with slope $\alpha_V = 2$ corresponding to virialised homologous systems has been plotted. Remnant mergers have been artificially displaced to coincide with the 'zero-point' of the FP of the SDSS.

Lacey C. G., Cole S., 1993, MNRAS, 262, 627
 Levine S. E., Aguilar L. A., 1996, MNRAS, 280, L13
 Meza A., Navarro J. F., Steinmetz M., Eke V. R., 2003, ApJ, 590, 619
 Mihos, J. C., Hernquist L., 1996, ApJ, 464, 641
 Mo H. J., Mao S., White S. D. M., 1998, MNRAS, 295, 319
 Mobasher B., Guzmán R., Aragón-Salamanca A., Zepf S., 1999, MNRAS, 304, 225
 Naab T., Burkert A. 2003, ApJ, 597, 893
 Navarro J. F., Frenk C. S., White S. D. M., 1995, MNRAS, 275, 56
 Navarro J. F., Frenk C. S., White S. D. M., 1997, ApJ, 490, 493
 Nipoti C., Londrillo P., Ciotti L., 2003, MNRAS, 342, 501
 Pahre M. A., Djorgovski S. G., de Carvalho R., 1998, AJ, 116, 1591
 Peebles P. J. E., 1993, Principles of Physical Cosmology. Princeton U. P., Princeton.
 Power C., Navarro J. F., Jenkins A., Frenk C. S., White S. D. M., Springel V., Stadel J., Quinn T., 2003, MNRAS, 338, 14
 Press W. H., Schechter P., 1974, ApJ, 187, 425
 Press W. H., Teukolsky S. A., Vetterling W. T., Flannery B. P., 1992, Numerical Recipes. Cambridge U. P., New York.
 Sérsic J. L., 1968, Atlas de Galaxias Australes. Córdoba, Argentina.
 Shen S., Mo H. J., Shu C., 2002, MNRAS, 331, 251 (SMS)
 Strauss M., Willick J. A., Phys. Rep., 261, 271
 Syer D., Mao S., Mo H. J., 1997, astro-ph/9711160
 Springel V., Yoshida N., White S. D. M., 2001, New Astronomy, 6, 79
 Schweizer F., 1998, in Friedli D., Martinet L. and Pfenniger D., eds, Galaxies: Interactions and Induced Star Formation, Saas-

Fee Advance Course 26, Springer-Verlag, N. Y.
 Toomre A., 1997 in Tinsley B. M. and Larson R. B., eds, The Evolution of Galaxies and Stellar Populations. Yale Univ. Obs., New Haven, p. 401
 Trujillo I., Burkert A., Bell E. F., 2004, ApJ, 600, L39
 Velázquez H., Aguilar L. 2003, RMxAA, 39, 197
 Wright L. J., Ostriker J. P., Naab T., Efstathiou G. 2003, astro-ph/0310513
 White S. D. M., 1997, astro-ph/9702214

This paper has been typeset from a \TeX / \LaTeX file prepared by the author.